AD-A148 436 ADVANCED DEVELOPMENT OF AN ACTIVE NEUROMUSCULATURE RESPONSE TO MECHANICAL..(U) PENNSYLVANIA STATE UNIV UNIVERSITY PARK DEPT OF INDUSTRIAL AN.. A FREIVALDS

1/1

UNCLASSIFIED 31 OCT 84 AFOSR-TR-84-1091 AFOSR-83-0106 F/G 6/16 NL

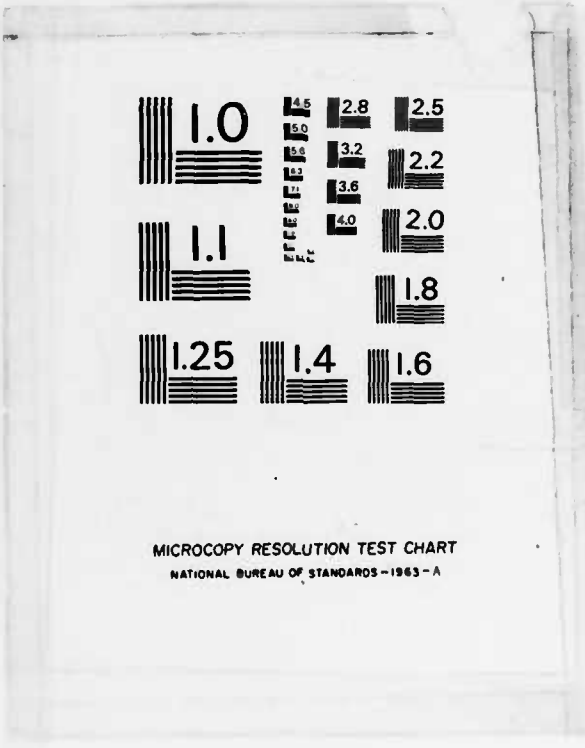
1.0
1.1
1.25
1.4
1.6
1.8
2.0
2.2
2.5
2.8
3.2
3.6
4.0
4.5
5.0
5.6
MICROCOPY RESOLUTION TEST CHART
NATIONAL BUREAU OF STANDARDS-1963-A

Final Report

ADVANCED DEVELOPMENT OF AN ACTIVE NEUROMUSCULATURE RESPONSE TO MECHANICAL STRESS

(AFOSR-83-0106)

by

Andris Freivalds
The Pennsylvania State University

1984 October 31

THE PENNSYLVANIA STATE UNIVERSITY
College of Engineering
Department of Industrial and
Management Systems Engineering
207 Hammond Building
University Park, Pa. 16802

11

Final Report

ADVANCED DEVELOPMENT OF AN ACTIVE NEUROMUSCULATURE RESPONSE TO MECHANICAL STRESS

(AFOSR-83-0106)

by

Andris Freivalds
The Pennsylvania State University

1984 October 31

REPORT DOCUMENTATION PAGE

1a. REPORT SECURITY CLASSIFICATION	1b. RESTRICTIVE MARKINGS
2a. SECURITY CLASSIFICATION AUTHORITY	3. DISTRIBUTION/AVAILABILITY OF REPORT Approved for public release; distribution unlimited.
2b. DECLASSIFICATION/DOWNGRADING SCHEDULE	
4. PERFORMING ORGANIZATION REPORT NUMBER(S)	5. MONITORING ORGANIZATION REPORT NUMBER(S) AFOSR-TR- 84-1091
6a. NAME OF PERFORMING ORGANIZATION The Pennsylvania State University 6b. OFFICE SYMBOL (If applicable)	7a. NAME OF MONITORING ORGANIZATION Air Force Office of Scientific Research
6c. ADDRESS (City, State and ZIP Code) University Park, PA 16802	7b. ADDRESS (City, State and ZIP Code) Building 410 Bolling AFB, DC 20332
8a. NAME OF FUNDING/SPONSORING ORGANIZATION 8b. OFFICE SYMBOL (If applicable)	9. PROCUREMENT INSTRUMENT IDENTIFICATION NUMBER AFOSR-83-0106
8c. ADDRESS (City, State and ZIP Code)	10. SOURCE OF FUNDING NOS. PROGRAM ELEMENT NO. 61102F; PROJECT NO. 2312; TASK NO. A1; WORK UNIT NO.
11. TITLE (Include Security Classification) Advanced Development of an Active Neuromusculature Response to Mechanical Stress	
12. PERSONAL AUTHOR(S) Andris Freivalds	
13a. TYPE OF REPORT Final 13b. TIME COVERED FROM 4/83 TO 10/84	14. DATE OF REPORT (Yr., Mo., Day) 1984 October 31 15. PAGE COUNT 62
16. SUPPLEMENTARY NOTATION (cont'd p 1)	
17. COSATI CODES FIELD / GROUP / SUB. GR.	18. SUBJECT TERMS (Continue on reverse if necessary and identify by block number) Biomechanics Biodynamic Models Neuromusculature

19. ABSTRACT (Continue on reverse if necessary and identify by block number)

An active neuromusculature response to mechanical stress was further developed. The basic mechanisms of muscle contraction at the fiber level, including the length-tension relationship, the force-velocity relationship and the active state function were re-examined. The basic fiber mechanisms were integrated into muscle systems utilizing motor unit organization, orderly recruitment of motor units and adjustments in force due to fatigue. The complete muscle systems were then used to replicate the human neuromusculature of the trunk and neck and for the elbow, shoulder, hip and knee joints. Preliminary simulations were of the human response to high Gy (lateral) accelerations compared favorably to experimentally obtained values. This muscularized Articulated Total Body Model will serve as a useful cost effective tool for the study of air crew responses in high-G environments.

20. DISTRIBUTION/AVAILABILITY OF ABSTRACT UNCLASSIFIED/UNLIMITED ☐ SAME AS RPT. ☐ DTIC USERS ☐	21. ABSTRACT SECURITY CLASSIFICATION
22a. NAME OF RESPONSIBLE INDIVIDUAL	22b. TELEPHONE NUMBER (Include Area Code) 22c. OFFICE SYMBOL

UNCLASSIFIED

PREFACE

Research in this final report was performed under Air Force Office of Scientific Research Grant-83-0106 awarded to The Pennsylvania State University from April 15, 1983 to October 31, 1984. The Air Force program monitors were John E. Lineiter and William Barry at the Air Force Office for Scientific Research , Bolling AFB, DC. The author expresses his sincere thanks to Ints Kaleps, Cory Carroll and Thomas Gardner, Modelling and Analysis Branch, Biodynamics and Bioengineering Division, Air Force Aerospace Medical Research Laboratory, Wright Patterson AFB, Ohio, for their suggestions, evaluations and patient assistance.

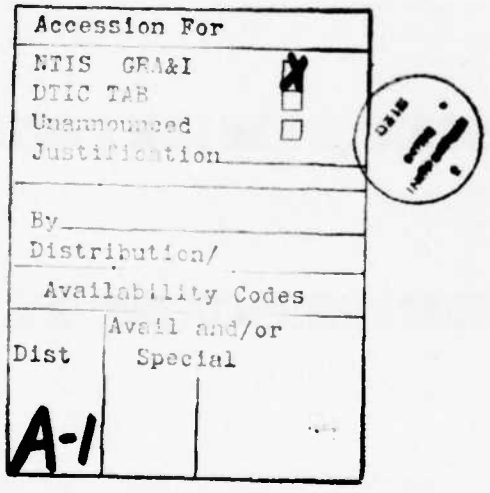

TABLE OF CONTENTS

LIST OF FIGURES

LIST OF TABLES

LIST OF SYMBOLS

A	=	cross-sectional area of muscle
B	=	viscous damping coefficient
BE	=	cross-bridge elastic element
CE	=	contractile element
DE	=	damping element
E	=	endurance time
f	=	force developed in muscle normalized by the maximum isometric tension
f_{DE}	=	force developed by damping element normalized by the maximum isometric tension
f_{ℓ}	=	force due to length-force relationship normalized by the maximum isometric tension
f_{PE}	=	force developed by parallel elastic element normalized by the maximum isometric tension
f_v	=	force due to force-velocity relationship normalized by the maximum isometric tension
F	=	force developed in muscle
F_{MAX}	=	maximum isometric tension
K_{PE}	=	spring constant for parallel elastic element
K_{SE}	=	spring constant for series elastic element
ℓ	=	instaneous muscle length
ℓ_0	=	resting muscle length
m	=	mass
n	=	relative number of recruited motor units
n_I	=	relative number of Type I motor units
n_{II}	=	relative number of Type II motor units
N	=	number of recruited motor units
N_I	=	number of Type I motor units

N_{II} = number of Type II motor units

$\bar{N}$ = total number of motor units

NF = functional form for muscle model

p = rate of change of active state

PE = parallel elastic element

PS = parallel elastic element of the sarcolemma

q = active state function

s = slack in muscle length

SE = series elastic element

t = time

t_c = contracation time of motor unit

γ = $\gamma_f - \gamma_o$

γ_o = resting Ca^{++} concentration

γ_f = free Ca^{++} concentration

ε = muscle strain

$\dot{\varepsilon}$ = muscle strain rate

$\dot{\varepsilon}_{MAX}$ = maximum muscle strain rate

ε' = pretensioned muscle strain

$\dot{\eta}$ = normalized muscle velocity

λ = length of contractile element

$\bar{\lambda}$ = resting length of contractile element

$\frac{\dot{\lambda}}{\lambda_0}$ = maximum shortening velocity of contractile element

λ_B = length of cross bridge elastic element

λ_S = length of series elastic element

μ = microns

ν = relative stimulation rate

ξ = normalized length of contractile element

τ^{-1} = stimulation rate

$\tilde{\tau}^{-1}$ = maximum stimulation rate

I. INTRODUCTION

Biodynamic computer-based models for the prediction of human body response to mechanical stress have become extremely useful and cost-effective research and developmental tools, especially as alternatives to direct experimentation with humans and animals. These models attempt to simulate or predict the forces and motions experienced by a body in high-acceleration events such as impacts or from sudden forces such as wind shear. In particular, the Air Force is interested in the reactions of aircrew personnel to such forces typically encountered in various phases of flight operations, including emergency ejections from high-speed aircraft. Such a hazardous environment is well suited to computer modeling, and with proper execution, considerable insight into body motion and stresses developed in the body can be gained.

The Modelling and Analysis Branch of the Biodynamics & Bioengineering Division of the Air Force Aerospace Medical Research Laboratory (AFAMRL) has been using a human body modelling computer program known as the Articulated Total Body (ATB) Model for several years. The model is based on rigid-body dynamics using Euler equations of motion with Lagrange-type constraints (Fleck et.al. 1974). The specific configuration uses 15 body segments (head, neck, upper torso, center torso, upper arms, lower arms, upper legs, lower legs, and feet) and 14 joints between the segments (Fleck and Butler, 1975). Although it was originally developed by the Calspan Corporation for the study of human-body and anthropometric-dummy dynamics during automobile crashes for the United States Department of Transportation (Fleck et.al. 1974; Fleck, 1975), the ATB Model was sufficiently general to allow simulation of whole-body articulated motion resulting from various impacts or abrupt accelerations applied to the body. Furthermore, modifications involving special joint

forces, aerodynamic forces and a complex harness system were added to accommodate specific Air Force applications (Fleck and Butler, 1975).

The ATB Model initially reflected human body structure, mass distribution and tissue material properties for passive responses. An early effort to improve the ATB Model in regards to active responses resulted in the development of a lumped three parameter viscoelastic muscle model superimposed on the advance restraint system. (Freivalds, 1984; Freivalds and Kaleps, 1983; Freivalds and Kaleps, 1984). However, the early efforts were constrained by the low number (five) of harness systems provided in the ATB Model, limiting simulations to simple joint motions or very crude whole body motion. Also, complex neuromuscular functions such as motor unit recruitment patterns, time varying effects, etc. were not included. Thus, further development of the neuromuscular system was needed to better simulate active human responses to high-g forces.

II. OBJECTIVES

The objective of this project was to further define and formulate methodologies for implementing active muscle responses into the present ATB Model. Two considerations were involved: (1) basic muscle phenomena such as motor units, recruitment patterns, and fatigue were to be included and (2) particular emphasis was to be placed on muscles acting in the torso and neck region which affect flexion, extension and lateral motion of the trunk in a seated posture.

The objective was approached in four-phased approach. In Phase I, the basic muscle model developed during the early efforts (Freivalds, 1984), was re-examined and redefined. In Phase II, advanced features of types of motor unit, motor unit recruitment, force buildup and endurance times were developed and included into the ATB Model. In Phase III, the ATB Model was modified to

allow for up to 50 muscles and a representative musculature for the entire body was developed. In Phase IV, various simulations were performed inorder to validate the modelling efforts.

III. BACKGROUND

A. Skeletal Muscle:

Skeletal muscles usually originate on the skeleton, span one or more joints and insert into a part of the skeleton again. Each muscle is enclosed in a connective tissue sheath called the epimysium and is held in its correct position in the body by layers of fascia. The muscle is attached to the bones via tendons, while the interior is compartmentalized into longitudinal sections called the fasciculi, each containing many individual muscle fibers. The fibers are enveloped by a connective tissue called the endomysium, which transmits the force of the muscle contraction from individual fibers to the tendons (Fung, 1981).

The muscle fibers do not always run parallel to the force transmitting tendons, as they do in fusiform muscles. They can be arranged in unipennate, bipennate or multipennate form, thus altering the force transmittinig characteristics (Fig. 1).

The muscle fiber, the basic structural unit, with a diameter of 10-60 μ and length from several millimeters to several centimeters, can be subdivided further into myofibrils of 1μ diameter. These myofibrils comprise the hexagonal array of protein filaments that are directly reponsible for the contractile process and give rise, with appropriate stains to the peculiar striations that are characteristic of skeletal muscle (Figure 2). A repeating unit known as the sarcomere is defined by the vertical z-disk. Two types of protein filaments are distinguishable in each sarcomere, thin ones about 5nm

Fig. 1 Schematic representation of skeletal muscle fibre arrangement.

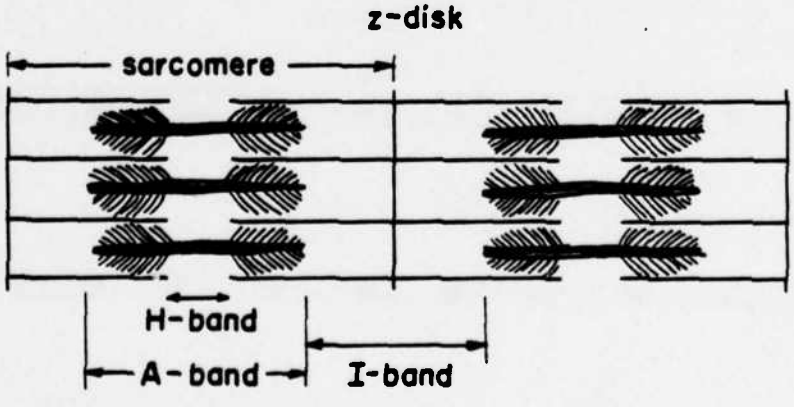

Fig. 2 Molecular substructure of mammalian skeletal muscle.

(50A) in diameter and thicker ones about 12nm (120A) across. The thin filaments contain actin, globular molecules in a triple helix, while the thick filaments contain myosin, long molecules with globular heads. The thin filaments are each attached at one end to a z-disk and are free at the other to interlace with the thick filaments. The A-band is the region of overlap between thick and thin filaments, the I-band contains solely the thin filaments, while the H-band is the middle region of the A-band into which the actin filaments have not penetrated (Fung, 1981).

The actual contractile process takes place at the junctions between the myosin and actin in a process known as the sliding filament theory first presented by H. E. Huxley (1953). The myosin molecules consist of a long tail piece and a "head". The tails lie parallel in a bundle to form the core of the thick filament while the heads project laterally from the filament in pairs, rotated with respect to its neighbors to form a spiral pattern along the filament. These heads seem to be able to nod; they lie close to their parent filament in relaxation, but stick out to actin filaments when excited. Thus, during muscle contraction the muscle fiber shortens as the filaments slide over each other, forming, breaking and reforming chemical bonds between the myosin heads and the globular actin molecules.

B. Previous Neuromuscular Modelling Efforts:

Previous modelling efforts (Freivalds, 1984; Freivalds and Kaleps, 1983; Freivalds and Kaleps, 1984) produced the lumped model of skeletal muscle shown in Figure 3. Structures which lie in parallel to the force producing sarcomeres: the sarcolemna (sheath) of the individual fiber and the various outer connective sheaths (fascia, endomysia, perimysia) are represented by the parallel elastic element (PE). Practically all the tension observed when stretching the resting muscle will result from this element. Because the

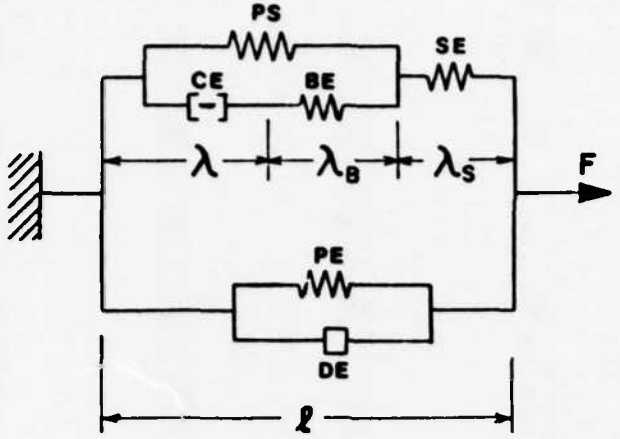

Fig. 3 Lumped model of skeletal muscle.

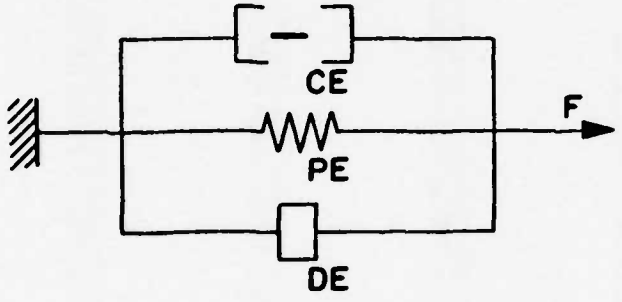

Fig. 4 Simplified muscle model.

muscle fiber is 60% water, an appropriate damping element (DE) is also included parallel to the contractile elements (CE). The contractile element represents the purely contractile protein molecules. In series with the contractile element is a bridge element (BE) representing the elastic elements within the cross bridges and the z-disks. The parallel elastic element for the sarcomere (PS) does not contain a damping component, since the sarcolemna attached to the z disks does not allow appreciable movement. The tendinous parts of the muscle fiber are located near the origin and insertion of the fiber and thus are depicted by a series elastic element (SE). Any mass of the sarcomeres is disregarded, especially when compared to the much larger external mass that the muscle contraction must move (Hatze, 1981).

The functional form of a harness within the advanced restraint system (Butler and Fleck, 1980) was utilized in representing the muscle

$$F(\varepsilon,\varepsilon') = F_1(\varepsilon) + F_2(\varepsilon)F_3(\varepsilon') + F_4(\varepsilon') \qquad (1)$$

where ε=strain, ε'=strain rate and F=total force. Obviously, from the functional form of Equation 1, only three elements can be modelled adequately. Furthermore, all three of these have to be in parallel, since forces in viscoelastic theory add directly only in parallel. Series elements would have required complex integro-differential equations which could not have replicated with out extensive changes to the model. However, certain assumtions allow a fairly easy reduction of the lumped model to a simpler form fitted by Equation 1. SE and BE can be considered to be very stiff springs and eliminated completely. This contention is supported by Bawa et.al. (1976) who found K_{SE}=3724 N/m to be much large than K_{PE}=1000 N/m. K_{BE} can be considered to be in a similar range with K_{SE}. Eliminating SE and BE results

in a model with four parallel elastic elements. These can be combined into one parallel elastic element, yielding the final simplified model in Figure 4.

The total force developed by the simplified model of Figure 4 can now be expressed as:

$$F = (f_{PE} + f_{CE} + f_{DE})F_{MAX} \tag{2}$$

where F_{MAX} is the maximum isometric tension of the muscle. Equation 2 corresponds very nicely with Equation 1 with:

$$\begin{aligned} f_{PE}\, F_{MAX} &= F_1(\varepsilon) \\ f_{CE}\, F_{MAX} &= F_2(\varepsilon)\, F_3(\dot{\varepsilon}) \\ f_{DE}\, F_{MAX} &= F_4(\dot{\varepsilon}) \end{aligned} \tag{3}$$

where

$$\begin{aligned} F_2(\varepsilon) &= f_\ell(\varepsilon) \\ F_3(\dot{\varepsilon}) &= f_v(\dot{\eta}) \end{aligned} \tag{4}$$

For concentric or shortening contractions f_{PE} is zero (PE producing force only under stretch) while f_{DE} produces a force opposite in sign to the contractile force. For eccentric or lengthening contractions, f_{PE} and f_{DE} all act in the same direction as f_{CE}.

Mathematical representations for each element were determined as follows. For the parallel elastic element, extensive tests on the tensile properties of resting human sartorius muscle carried out by Yamada (1970) indicate an exponential force-strain function:

$$f_{PE} = .0016296(e^{7.6616\varepsilon-1}) \tag{5}$$

where f_{PE} is the force developed by the PE normalized with respect to maximum isometric tension in the muscle and ε is the strain:

$$\varepsilon = \frac{\ell-\ell_o}{\ell_o} \tag{6}$$

where ℓ is the instananeous muscle length and ℓ_o is the resting length. This force-strain curve is shown in Figure 5.

The velocity dependence of the damping element (DE) can be expressed similarly to the form used for a simple mechanical dashpot:

$$f_{DE} = .00588\,\dot{\varepsilon} \tag{7}$$

where f_{DE} is the normalized force and $\dot{\varepsilon}$ is the muscle strain rate. This curve is shown in Figure 6.

The contractile element is the only active component in the model. Its behavior is extremely complex and depends nonlinearly on its length, contractive history, velocity of movement, the degree of stimulation and its temperature. However, for practical purposes, only the basic functions were considered: the length-force relationship and the force-velocity relationship.

The length-force relationship is determined by the number of active cross links or filamentary overlap and can be adequately expressed from the data of Gordon et.al. (1966) by the functional suggested by Hatze (1981, p. 42):

$$f_{\ell}(\varepsilon) = .32 + .71e^{-1.112\varepsilon}\sin(3.722(\varepsilon+.344)) \tag{8}$$

This function is shown in Figure 7.

Fig. 5 PASSIVE MUSCLE FORCE
– STRAIN FUNCTION

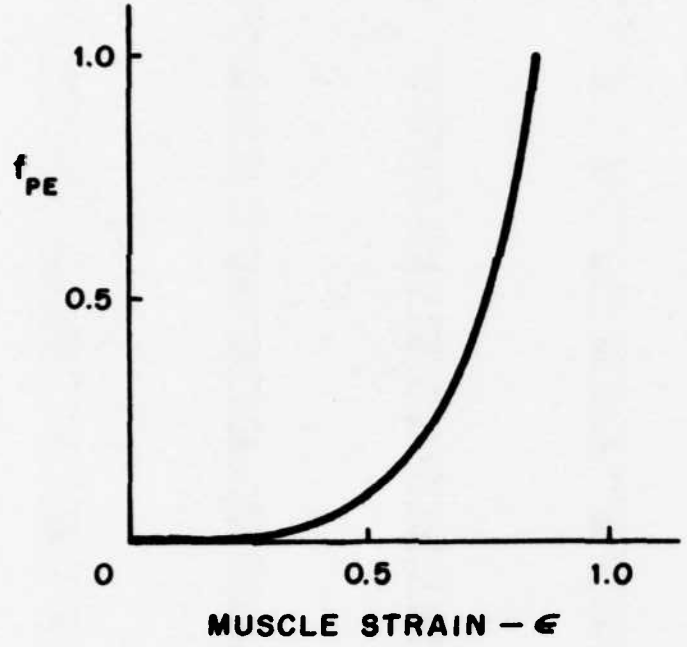

Fig. 6 PASSIVE MUSCLE VISCOUS DAMPING FORCES

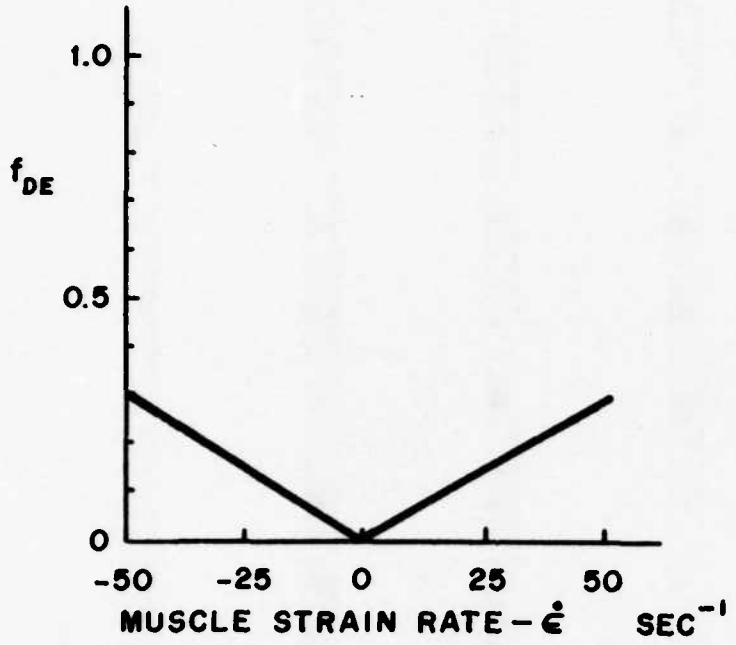

Fig. 7 MUSCLE LENGTH-FORCE RELATIONSHIP

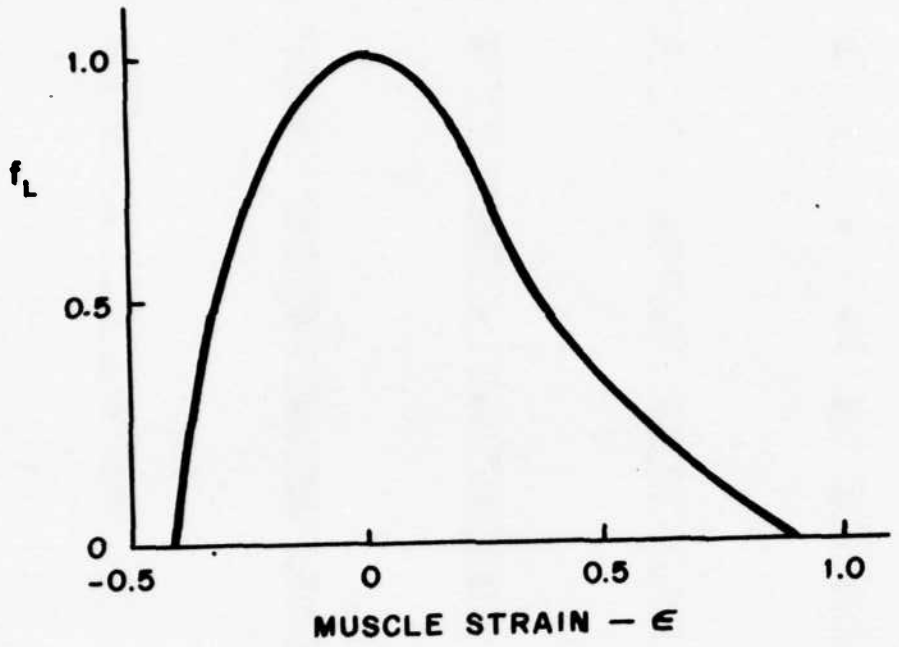

The force-velocity relationship is determined by the rate of breaking and reforming the cross bridges with higher rates producing less effective bonds. To account for the whole range of negative velocities (shortening or concentric contractions) as well as positive velocities (lengthening or eccentric contractions) Hatze (1981, p. 45-46) has defined the following expression:

$$f_v(\dot{\eta}) = .1433\ \{.1073 + e^{-1.409}\ \sinh\ (3.2\dot{\eta} + 1.6)\}^{-1} - .005[2-e^{6\varepsilon}] \qquad (9)$$

where $f_v(\dot{\eta})$ is the normalized force due to the force-velocity relationship as defined by the first term and reduced by internal resistance as defined by the second term. However, since the coefficient of the second term is smaller by a factor of 30 than the first term, it can be disregarded for present purposes. $\dot{\eta}$ represents the normalized contractile element velocity:

$$\dot{\eta} = \dot{\varepsilon}/\dot{\varepsilon}_{MAX} \qquad (10)$$

with $\dot{\varepsilon}_{MAX}$ being the maximum shortening velocity of the contractile element. Equation 6 represented by Figure 8.

IV. PHASE I - REDEFINITION OF THE BASIC MUSCLE MODEL

A. Passive Viscoelastic Elements:

Previous efforts to define a neuromuscular response with the ATB Model utilized simulations of elbow-flexion (Freivalds, 1984; Freivalds and Kaleps, 1983). These indicated several conclusions. The passive strain function as represented by f_{PE} produced an insignificant increment to the total muscle force even with 15% strain at complete extension of the forearm. This was

Fig. 8 MUSCLE FORCE–VELOCITY RELATIONSHIP

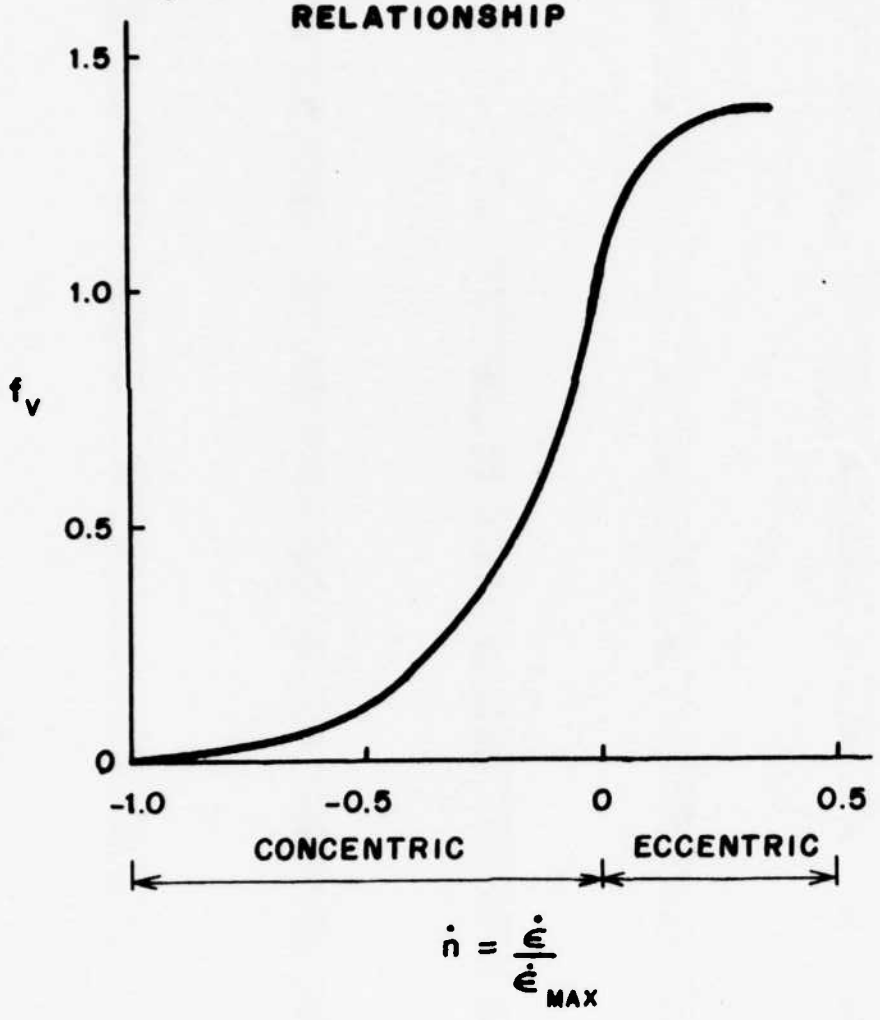

B. Active State Function:

The action of the contractile element is more complex than initially modelled. Not only is the force production dependent on the length of the muscle fiber and the velocity of contraction but also on the active state q of the muscle fiber. This active state q is defined as the relative amount of Ca bound to troponin (inhibitor molecule of actin). If the maximum number of potential interactive sites on the thin filament are exposed by the action of Ca^{++}, then q=1; while in a resting state $q=q_o$. Thus the isometric tension developed by a muscle fiber at a given length ℓ_q the CE is directly proportional to q (Hatze, 1981, p. 33).

Define γ to be the difference between the real free Ca^{++} concentration γ_f and the free Ca^{++} concentration γ_o in the resting fiber. However, for practical purposes since $\gamma_o << \gamma_f$, we have $\gamma=\gamma_f$. Let $p = dq/d\gamma$ denote the Ca^{++} concentration rate of change of the active state q. The process of binding Ca^{++} ions to the troponin sites is hypothesized by Hatze (1981) and supported by the experimental studies of Ebashi and Endo (1968) to be a function of the length ℓ of the CE and of the difference between the maximum and present value of q and controlled by a negative feedback loop as follows.

$$dp/d\gamma = \rho_1^2(\varepsilon)\ (1-q)-2\rho_2\rho_1(\varepsilon)p \qquad (8)$$

where $\varepsilon = (\ell-\ell_o)/\ell_o$ is the strain and

$$dq/d\gamma = p \qquad (9)$$

Solving the differential system of Equation 8 and Equation 9 with initial conditions:

$$p(0) = 0$$

above 50% strain. Reductions in force levels due to the active length-force relationship were larger amounting to approximately a 16% reduction of the maximum voluntary contraction (MVC) at full flexion and a 10% reduction at full extension. The force velocity curve showed as much as 30% changes in force production levels.

The force produced by the passive viscous damping element amounted to as much as a 30% increase above MVC. This seemed to be an excesesively large effect for a passive response and consequently the damping coefficient was re-evaluated. Glantz (1974) derived a damping coefficient of $5(g/mm^2)/(mm/sec)$ using the data of isolated cat papillary (cardiac) muscle of length 8.5mm from Parmley et.al (1970). This value was normalized to a more useful unitless value of .00588 expressed as fractional force per velocity of muscle lengths/second. Force was normalized by the maximum muscle strength of 100 N per cm^2 of muscle cross-sectional area. This seems to be the upper limit of inherent muscle strength as determined by a wide range of researchers using different techniques (Fick, 1910; Ikai and Fukunga, 1968; Hatze, 1981). Velocity was normalized by the muscle specimen length of 8.5mm such that the f_{DE} calculation could be used regardless of muscle type or length. This unknown factor in the previous deviation (Freivalds, 1984) was probably the main cause of the unusually large values of damping forces. A final assumption necessary to complete the calculation of the damping coefficients is that the coefficient for skeletal muscle would be similar in value to that of cardiac muscle. Since coefficients for skeletal muscle have not been calculated, no other alternative is available.

$$q(0) = q_o = .005 \tag{10}$$

One obtains a normalized solution:

$$q(\varepsilon,\gamma) = 1 - \frac{(1-q_o)}{(m_1-m_2)} \left\{ m_1 e^{m_2\rho_1(\varepsilon)\gamma} - m_2 e^{m_1\rho_1(\varepsilon)\gamma} \right\} \tag{11}$$

where

$$m_{1,2} = -\rho_2 \pm (\rho_2^2 - 1)^{1/2} \quad \rho_2 > 1 \tag{12}$$

Substituting experimentally found values (Hatze, 1981):

$$\rho_1^2 = 2.34 \times 10^{14} \left(\frac{\varepsilon+.44}{\varepsilon+1}\right)^{1/2} \quad -.44 \leq \varepsilon \leq .8 \tag{13}$$

$$\rho_2 = 1.05$$

One obtains:

$$q(\varepsilon,\gamma) = 1 - (1-q_o)(2.14\, e^{-1.167 \times 10^7\, h(\varepsilon)\gamma(t)} - 1.14 e^{-2.096 \times 10^7 h(\varepsilon)\gamma(t)}) \tag{14}$$

where

$$h(\varepsilon) = \left(\frac{\varepsilon+.44}{\varepsilon+.1}\right)^{1/2}$$

However, a simple computational approximation is provided by Hatze (1981, p. 40) for most mammualian muscles:

$$q(\varepsilon,\gamma) = \frac{q_o+\rho^2(\varepsilon)\gamma^2}{1+\rho^2(\varepsilon)\gamma^2} \tag{15}$$

where

$$\rho(\varepsilon) = 66{,}200\ \frac{1.9(\varepsilon+1)}{1.9 - \varepsilon} \tag{16}$$

The function Υ, the free Ca^{++} ion concentration can be represented as a function of time t and the stimulation rate ν by a trend function which represents the average behavior of Υ in successive time intervals, and which approaches a maximum value asymptotically and has the rate of increase proportional to the stimulation rate (Hatze, 1981, p.39).

$$\dot{\Upsilon} = m(C\nu - \Upsilon) \quad \Upsilon(0) = \Upsilon_o \tag{17}$$

where m and c are constants ($C = 1.373 \times 10^4$ (Hatze, 1981) and m to be determined later) and ν is the relative stimulation rate defined by

$$0 \leq \nu = \frac{\tilde{\tau}}{\tau} \leq 1 \tag{18}$$

where τ^{-1} and $\tilde{\tau}^{-1}$ denote the stimulation rate and maximum stimulation rate respectively.

The rate of stimulation of motor units during voluntary contraction has been very controversial. Several studies have found a fairly constant discharge frequency over a wide range of tension for individual motor units (Bigland and Lippold, 1954; Clamann, 1970), while others maintain that an increase in muscle tension is achieved in part by an increase in the stimulation rate and that this may be important in achieving precision and smoothness of contraction (Marsden et.al 1971; Person and Kudina, 1972; Milner-Brown et.al 1973). However, even for those studies who found a rise in discharge frequency with tension, the frequency at the start of the discharge for rapid contractions was much higher and closer to the maximum stimulation rate (Tanji and Kato, 1973). Thus, it is fairly reasonable to assume a

constant stimulation rate and, therefore, a constant relative stimulation rate.

Now solving Equation 17 with ν constant yields:

$$\gamma = (\gamma_o - C\nu)\, e^{-mt} + C\nu \tag{19}$$

With $\gamma_o << C\nu$ ($\gamma_o = 1 \times 10^{19}$; Hatze, 1981), Equation 19 reduces to:

$$\gamma = C\nu(1-e^{-mt}) \tag{20}$$

Substituting Equation 20 and Equation 16 into Equation 15 yields (Figure 9):

$$q(t) = \frac{.005 + 82.63\ \nu^2\ (1-e^{-mt})^2}{1 + 82.63\ \nu^2\ (1-e^{-mt})^2} \tag{21}$$

Consequently, f_{CE} can be redefined by using the relative force f_q developed by the active state function q:

$$f_{CE} = f_q(t)\ f_\rho(\varepsilon)\ f_v(\dot{n}) \tag{22}$$

IV. PHASE II - ADVANCED DEVELOPMENT

A. Organization of Fibers into Motor Units

The population of motor units can be subdivided into two distinct populations based on their contractile and histochemical properties: Type I (slow twitch) motor units and Type II (fast twitch) motor units (Close, 1972). Type I motor units have slower contraction times, tend to be more aerobic and less fatigable and are recruited at lower tension levels. Type II motor units have faster contraction times, tend to be more anaerobic and more fatigable and are recruited at higher tension levels (Close, 1972; Milner - Brown,

Fig. 9 RELATIVE FORCE DEVELOPED BY ACTIVE STATE FUNCTION VS. TIME

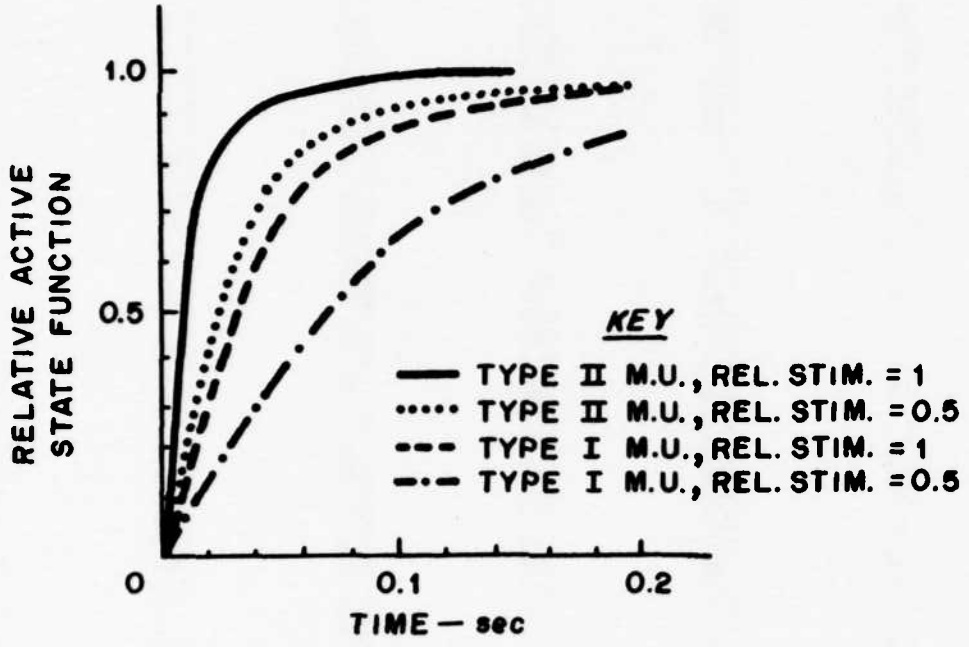

et.al., 1973). Thus, the total muscle force output should be the sum of the force output from N_I of the Type I motor units and N_{II} of Type II motor units:

$$F = (f_{PE} + f_{CE_I} + f_{CE_{II}} + f_{DE})F_{MAX} \tag{23}$$

Furthermore, the same total population can be subdivided into two-dynamically different populations: the N population of active motor units and the $\bar{N}$-N population of inactive or resting motor units, where $\bar{N}$ is the total number of motor units in the muscle.

Muscle properties dependent on fiber type will be developed in the next section as many of these also depend on the recruitment pattern used.

Orderly Recruitment of Motor Units

It has been well established that motor units are recruited in a sequential order according to their sizes (Milner - Brown, et.al. 1973). The cumulative relative cross-sectional area u occupied by the fibers of the recruited units increases by:

$$u = u_o e^{\bar{c}\frac{(N-1)}{\bar{N}}} \qquad o < u_o < u \leq 1 \tag{24}$$

where

$$\bar{c} = -\ell n\, u_o,$$

N is the number of stimulated motor units and $\bar{N}$ is the total number of motor units (Hatze, 1979). For $\bar{N}$ large, Equation 24 reduces to:

$$u_n = u_o e^{\bar{c}N/\bar{N}} = u_o(1-^{N}/_{\bar{N}}) = u_o^{(1-n)} \tag{25}$$

where n is the normalized number of recruited or active motor units = $^{N}/_{\bar{N}}$.

The $\Delta_i u$ of the relative cross-sectional area u upon recruitment of the i^{th} motor unit is then defined by:

$$\Delta_i u = C\, e^{\bar{c}i/\bar{N}} \tag{26}$$

where C is a normalization constant determined by the requirement that

that $\sum_{i=1}^{\bar{N}} \Delta iu = 1$ i.e.

$$C = \frac{1}{\sum_{i=1}^{N} e^{\bar{c}i/\bar{N}}} \tag{27}$$

Applying the ratio of the smallest to the largest motor unit potential measured in a muscle to Equation 25, an estimate of the value of u_o for a given muscle can be found. These range from u_o=.005 for the human rectus femorus muscle to u_o=.009 for the human biceps muscle (Hatze, 1979) with an average value of u_o=.00673 resulting in c=5 to be used for the present study.

Thus two very important properties of motor unit recruitment dynamics have been included; motor units are normally recruited sequentially from the smallest to the largest and the size of the recruited units grown exponentially. Combining the two sets of overlapping population distribution of motor units yields two distinct cases: a) $N < N_I$, ie. only part of the Type I motor units are stimulated and none of the Type II can be stimulated

because of the orderly recruitment pattern and b) $N > N_I$, ie., all Type I motor units are stimulated and some of the Type II motor units are stimulated, but none of the Type I are inactive. These conditions can be expressed mathematically by adjusting f_{CE} by the motor unit type and the relative area of the number of motor units recruited. Since the force developed in a muscle is directly proportional to the area stimulated (Ikai, M. and Fukunga, T. 1968). Thus for $0 \leq n \leq n_I$ where $n_I = \frac{N_I}{\bar{N}}$

$$a)\ f_{CE_I} = f_{q_I}(t)\ f_{\ell_I}(\varepsilon)\ f_{v_I}(\dot{n})\ u_o^{(1-n)} \tag{28}$$

and for $n_I \leq n \leq 1$

$$b)\ f_{CE_I} = f_{q_I}(t)\ f_{\ell_I}(\varepsilon)\ f_{v_I}(\dot{n})\ u_o^{(1-n_I)}$$

$$f_{CE_{II}} = f_{q_{II}}(t)\ f_{\ell_{II}}(\varepsilon)\ f_{v_{II}}(\dot{n})\ [u_o^{(1-n)} - u_o^{(1-n_I)}] \tag{29}$$

Equation 28 and 29 can be substituted directly into Equation 23 for the overall definition of muscle force. f_{PE} and f_{DE} are determined by the total cross-sectional area of the muscle, whether all motor units are completely recruited or not. One further adjustment is to substitute

$$F_{MAX} = kA \tag{30}$$

into Equation 23. The maximum isometric tension for any skeletal muscle is determined by the inherent muscle strength per cross sectional area k (k = 100 N/cm^2 as determined by Fick, 1910; Ikai and Fukunga, 1968; Hatze, 1981) multiplied by the cross-sectional area of the muscle A (Figure 10).

Fig. 10 FORCE DEVELOPED BY ORDERLY RECRUITMENT OF MOTOR UNITS

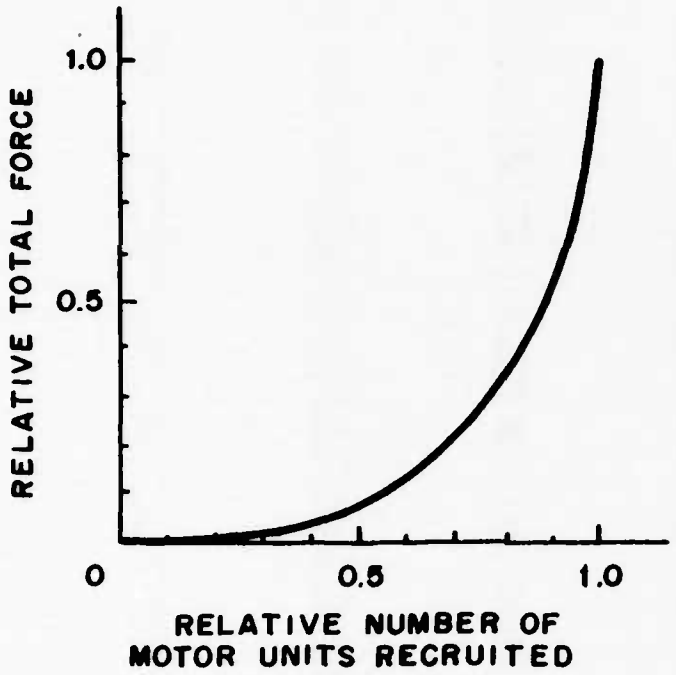

Additional properties of motor units can be obtained from the data presented in Henneman and Olson (1965). The contraction time t_c of a motor unit is a decreasing function of the fraction n of recruited motor units:

$$t_c = a_2 - a_3 n \tag{31}$$

Thus for Type I motor units

$$t_{c_I} = a_{2_I} - a_{3_I} n \qquad 0 \leq n_I \leq n_I \tag{32}$$

and for Type II motor units

$$t_{c_{II}} = a_{2_{II}} - a_{3_{II}} n \qquad n_I \leq n \leq 1 \tag{33}$$

The constants a_{2_I}, a_{3_I}, $a_{2_{II}}$, $a_{3_{II}}$ can be determined from experimental values. For n=0, the value of t_c corresponds to the contraction time of the slowest Type I unit in the muscle, approximatley equal to .1 sec.; for $n=n_I$ the value of t_c corresponds to the fastest Type I unit, approximately .045 sec.; and for n=1 (given $n_I \neq 1$) the value of t_c corresponds to the fastest Type II unit, approximately .02 sec. (Stephens and Stuart, 1975). Substituting and solving for the unknown values yields:

$$\begin{aligned} a_{2_I} &= .1 \\ a_{3_I} &= .055/n_I \\ a_{2_{II}} &= .02 + \frac{.025}{(1-n_I)} \\ a_{3_{II}} &= \frac{.025}{(1-n_I)} \end{aligned} \tag{34}$$

Substituting Equation 34 into Equation 32, 33 yields

$$t_{C_I} = .1 - \frac{.055\, n}{n_I} \tag{35}$$

$$t_{C_{II}} = .02 + \frac{.025\, 1-n}{1-n_I} \tag{36}$$

Several other important parameters can be derived using Equation 31. Close (1965) showed that for mammalian skeletal muscle the maximum normalized speed of shortening is related to the contraction time of a muscle, consisting predominantly of one fiber type, by:

$$\dot{\varepsilon}_{MAX} = \frac{B}{t_c} \tag{37}$$

where B has a value of .297 for human muscle. Using Equation 35 and 36, $\dot{\varepsilon}_{MAX}$ is found to be 2.97/sec. for slow (n=0) and 14.85/sec. for fast (n=1) motor units. However, for present modelling purposes, an average value for $\dot{\varepsilon}_{MAX}$ will be used. Integrating t_c from Equation 35 over the pattern of motor of motor unit recruitment:

$$\frac{\int_0^n \left(.1 - \frac{.055x}{n_I}\right) e^{cx} dx}{\int_0^n e^{cx} dx} \tag{38}$$

yields:

$$\frac{.1\,(e^{cn}-1) - \frac{.055}{cn_I}\, e^{cn}(cn-1)-1}{e^{cn}-1} \tag{39}$$

A Similar process is used for $t_{c_{II}}$ in Equation 36.

The rate constant in Equation 19 also depends on the contraction time:

$$m = A_o/t_c \tag{40}$$

where A_o = .372 for human muscle (Hatze, 1981, p. 62) For slow motor units (n=0) m = 3.72 and for fast motor units (n=1) m = 18.5. Again an average value is used for present modelling efforts.

Time Varying Effects

The most important time varying effect in the muscle is fatigue. It is obvious that people can maintain their maximum effort very briefly (5 seconds), whereas they can maintain a force of around a quarter of their maximum strength for an extended period of time. Such an endurance responses can be explained by examining the properties of individual motor units. Type I motor units tend to be more aerobic, less fatigable and are recruited at lower tension levels. While Type II motor units tend to be an aerobic, more fatigable and are recruited at higher tension levels, (Stephens and Usherwood, 1977). Although exact fatigue and recovery patterns for individual motor units have not been identified, the maximum endurance time can be estimated from experimental studies. The earliest experiments of Miller (1932) implied that the length of time a force could be maintained depended on the fraction of available strength to be exerted. This relationship was further verified by Rohmert, 1960, Kogi and Hakamada, 1962; Caldwell 1963, 1964; Monod and Scherrer, 1965; Schutz, 1972. Only three studies attempted to derive and publish formulas of this relationship. Monod and Scherrer (1965) proposed:

$$E(\text{min}) = \frac{2.5}{((\%F_{MAX}-14)/100)^{2.4}} \quad (41)$$

Kogi and Hakamada (1962) suggested

$$E(\text{min}) = \frac{5012}{(\%F_{MAX})^{1.99}} \quad (42)$$

while Schutz (1972) indicated:

$$E(\text{min}) = -1.25 + \frac{1.25}{\%F_{MAX}} \quad (43)$$

All of these formulas have some faults that limit their usefulness in representing the empirical data. Equation 42 and 43 do not account well for the asymptotic relationship of endurance approaching indefinite times for force levels of 15-20% MVC, Equation 41 does provide the asymptote but predicts lower than normal endurance times for large force levels. A separate formula was developed for the current work, based on the data of Rohmert (1960), who, with over 300 subjects tested, had the largest sample size. Best fit was produced by the hyperbolic relationship (shown in Figure 11):

$$E(\text{sec}) = \frac{1236.5}{(\%F_{MAX}-15)^{.618}} - 72.5 \quad (44)$$

Once the endurance time is exceeded, however, the person's strength does not immediately fall to zero. For maximal or large submaximal efforts, there is still a gradual decay to the lower level of 15-20 percent found for indefinite holds (Petrofsky, 1982, p. 55). This experimental data can be modelled very easily using polynomial regression:

Fig. 11 ENDURANCE TIME AS A FUNCTION OF RELATIVE STRENGTH

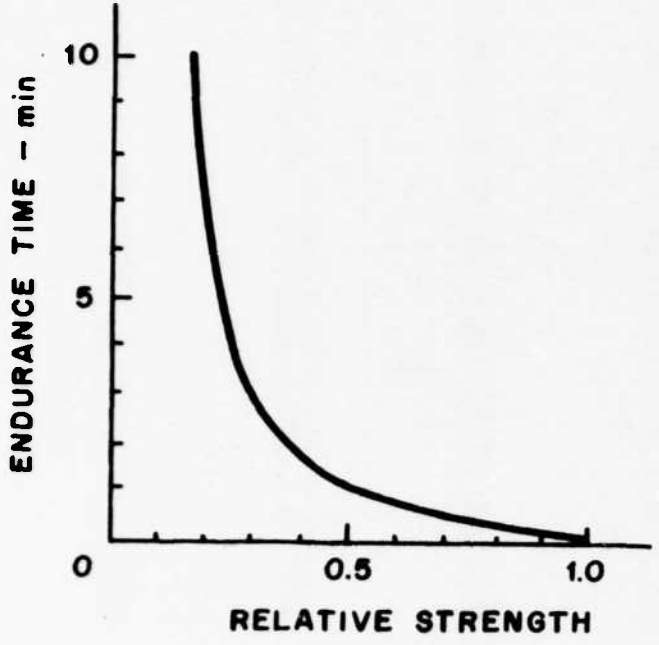

$$\%F = 98.1 - 23.9t + 1.9t^2 \quad (45)$$

VI. PHASE III - MODELLING THE GENERAL MUSCULATURE

The attachment of the complete muscle systems to limb segments, includes the identification of joint biomechanics, the measurement of origin and insertion distances, the integration of agonist and antagonist actions and computation of cross-sectional areas for estimation of total force production. Methods to accomplish this can be best described according to the joints or area of the body involved.

A. Elbow Joint:

Modelling of the elbow and simulation of elbow flexion is perhaps the easiest case to examine and will serve as a simple example demonstrating the validity of the technique used for the more complicated joints. The model includes two segments: the humerus, and a combination of the ulna and the radius and three elbow flexor muscles: biceps brachii, brachialis and brachioradialis. Examination of the biceps brachii more closely shows the origin of the long head to be at or beyond the gleno - humeral joint (Mc Minn and Hutchings, 1977). The insertion can be set at approximately 3.5 cm from the elbow joint corresponding to the data of Wilkie (1950). Using the cross-sectional area of 4.58 cm^2 for the biceps (Schumacher and Wolff, 1966) and multiplying by the maximum muscle force of 100N/cm^2 (Hatze, 1981) yields a maximum isometric tension of 458 N. (The difference between anatomic and physiological areas due to fiber- orientation are accunted for). Adding the force of 690N generated by the brachialis (6.9 cm^2 x 100 n/cm^2) to the biceps yields a maximum elbow flexion force of 1148 N. Such a value can be compared to the data of Wilkie (1950) who found that his subjects could maintain a maximum of 195.8 N at the wrist. With a lever ratio between muscle insertion

distance and the moment arm of the weight of .15, the maximum elbow flexion force is 1305 N. These values are remarkably close considering that other minor muscles producing additional torgue are not accounted for in the first calculation. Similar calculations were conducted on the other muscles.

Complete details on all of the elbow muscles are based on previously collected data (Chao and Morrey, 1978; Youm, et.al. 1979; Maton, et.al. 1980; Amis, et.al., 1980; Hatze, 1981) and are summarized in Table 1.

B. Shoulder Joint:

The shoulder is a much more complicated joint consisting of three separate joints: the glenohumeral joint, the acromioclavicular joint and the sternoclavicular joint. Correspondingly, many more muscles are involved to produce many different actions. Details on the actions of these muscles, points of origin and insertion, along with cross-sectional areas are taken from previous biomechanical studies (Schumacher and Wolff, 1966; Dempster, 1965; DeLuca and Forrest, 1973; Engin, 1980) and given in Table 2.

C. Hip Joint and Knee Joint:

Although consisting of only one joint, the hip is a ball and socket joint and along with the many muscles involved, undergoes many different types of actions. A further complication is that a majority of these muscles span both hip and knee joints and thus hip actions cannot be uniquely separated form knee actions. Details on the actions of these muscles, points of origin and insertion, along with the cross-sectional areas were taken from earlier biomechanical studies (Merchant, 1965; Schumacher and Wolff, 1966; Seireg and Arvikar, 1973; Jensen and Davy, 1975; Crowninshield, et.al. 1978; Dostal and Andrews, 1981; Smidt, 1973; Nissan, 1980; Wismanis, 1980; Minns, 1980) and are summarized in Table 3.

D. Trunk and Neck Musculature:

Simulation of the trunk musculature is a much more difficult undertaking than for the previous joints. First of all, there are many muscles involved, close to 20 major ones for the lower back and trunk and equally many for the neck region. Secondly, some of the muscles, such as the longus, spinalis and semispinalis, have many attachment sites between the different vertebrae. Thirdly, the lines of action of the muscle forces are not always in straight line, e.g., the interior and exterior obliques. Fourthly, the vertebral joints are complicated by the ligaments and their additional force-bearing capabilities. Appropriate approximations were used when necessary.

Details on insertions and origins were obtained from Rab et.al. (1977), Rab (1979), Takashima, et.al. (1979), and Williams and Belytschko (1981), while cross-sectional areas were used from Schumacher and Wolff (1966) and Williams and Belytschko (1981). A summary of these findings is given in Tables 4 (neck) and 5(trunk).

Table 1 Specifications on Elbow Musculature

Muscle Group	Origin	Insertion	Action	Cross-Sectional Area (cm2)
Biceps brachii	Short head from coracoid process of scapula, long head from supraglenoid tuberosity	Radial tuberosity	Flexion of forearm	3.55
Brachialis	Lower anterior surface of humerus	Coronoid tuberosity of ulna	Flexion of forearm	4.63
Brachioradialis	Proximal two-thirds of humerus	Styloid process of ulna	Flexion of forearm	1.37
Triceps brachii	Long head from infraglenoid tunerosity of scapula, lateral and medial head from posturior surface of humerus	Olecranon	Extension of forearm	16.38
Anconeus	Lateral epicondyle humerous	Olecranon	Extension of forearm	.94
Pronator teres	Medial epicondyle of humerus	Middle of radius	Pronation of forearm	1.61
Supinator	Lateral epicondyle of humerus	Laterial and anterior surface of radius	Supination of forearm	1.77

Table 2 Specifications on Shoulder Musculature

Muscle Group	Origin	Insertion	Action	Cross-Sectional Area (cm^2)
Deltoid	Clavicle, scapula acromion	Deltoid tuberosity of humerus	Abduction of arm	11.01
Supraspinatus	Supraspinous fossa of scapula	Greater tuberosity of humerus	Abduction of arm	3.3
Pectoralis major	Clavicle, Stermum	Bicipital groove of humerus	Adduction of arm	6.8
Latissimus dorsi	Lower Thoracic and lumbar vertebrae	Bicipital groove of humerus	Adduction of arm	5.37
Teres major	Inferior angle of scapula	Bicipital groove of humerus	Adduction of arm	4.97
Teres minor	Axillary border scapula	Greater tuberosity of humerus	Adduction of arm	1.57
Subscapularis	Subscapular fossa scapula	Lesser tuberosity of humerus	Flexion of arm	9.9
Coracobrachialis	Coracoid process scapula	Medial border of humerus	Flexion of arm	1.52
Infraspinatus	Infraspinous fossa of scapula	Greater tuberosity of humerus	Extension of arm	5.98

Table 3 Specifications on Hip and Knee Musculature

Muscle Group	Origin	Insertion	Action	Cross-Sectional Area (cm^2)
Gluteus medius	Iliac crest of pelvis	Greater trochanter of femur	Abduction of thigh	21.18
Gluteus minimus	Outer surface of ilium (pelvis)	Greater trochanter of femur	Abduction of thigh	9.6
Tensor fasiae latae	Anterior part of iliac crest of pelvis	Iliotibial tract of femur	Abduction flexion of thigh	2.48
Obturatus internus	Obturatus foramen area of pelvis	Greater trochanter of femur	Abduction of thigh	3.91
Adductor longus	Pubis of pelvis	Linea aspera of femur	Adduction flexion of thigh	5.03
Adductor brevis	Pubis of pelvis	Below lesser trochanter of femur	Adduction flexion of thigh	4.54
Adductor magnus	Ischial tuberosity of pelvis	Linea aspera of femur	Adduction flexion of thigh	20.58
Pectineus	Pubic tubercle of pelvis	Below lesser trochanter of femur	Adduction flexion of thigh	2.47
Quadratus femoris	Ischial tuberosity of pelvis	Quadrate tubercle of femur	Adduction of thigh	2.91
Obturatus externus	Obturator foramen area of pelvis	Trochanteric fossa of femur	Adduction of thigh	4.95
Gluteus maximus	Iliac crest of sacrum	Iliotibial tract of femur	Extension of thigh	29.42
Semimembranosus	Ischial tuberosity of pelvis	Upper part of tibia	Extension of thigh flexion of leg	12.97
Semitendinosus	Ischial tuberosity of pelvis	Medial condyle tibia	Extension of thigh flexion of leg	4.33

Table 3 (Continued)

Biceps femoris	Ischial tuberosity of pelvis, linea aspera of femur	Lateral condyle of tibia, head of fibula	Extension of thigh, flexion of leg	11.8
Quadriceps femoris	Iliac spine of pelvis anterion surface of femur	Patela	Flexion of thigh extension of leg	56.0
Iliopsoas	L2-L4 vertebral bodies, iliac fossa of pelvis	Lesser trochanter of femur	Flexion of thigh	15.06
Gastrocnemus	Medial and lateral condyles of femur	Calcaneus	Flexion of leg	15.66
Popliteus	Lateral condyle of femur	Posterior surface of tibia	Flexion and rotation of leg	1.99
Gracilis	Pubic symphysis of pelvis	Upper medial surface of tibia	Flexion of leg, adduction of thigh	1.63
Sartorius	Iliac Notch of oi' pelvis	Upper Medial surface of tibia	Flexion of leg and thigh	1.55

Table 4 Specifications on Neck Musculature

Muscle Group	Origin	Insertion	Action	Cross-Sectional Area (cm^2)
Longus Capitis	Transverse processes of C3, C4, C5, C6	Basilar part of occipital bone	Flexion of head	.75
Rectus capitis anterior	C1 transverse processes	Front of foramen magmum on occipital bone	Flexion and notation of head	.25
Rectus capitis lateralis	C1 transverse processes	Jugular process of occipital bone	Lateral flexion of head	.25
Rectus capitis posterior major	C2 spinous process	Inferior nuchal line of occipital bone	Extension, lateral flexion of head	.50
Rectus capitis posterior minor	C1 spinous process	Inferior nuchal line of occipital bone	Extension, laterial flexion of head	.385
Obliquus capitis superior	C1 transverse processes	Inferior nuchal line of occipital bone	Extension and lateral rotation of head	1.00
Splenius capitis	Spinous process of T1 and C7	Occipital bone and temporal bone	Extension and lateral flexion of head	1.22
Longissimus capitis	Transverse processes of T1, C6, C4	Mastoid process of Temporal bone	Extension and Lateral flexion of head	.5
Spinalis capitis	Transverse processes of T1 and C7	Between superior and inferior nuchal line of occipital bone	Extension and lateral flexion of head	.5
Semispinalis capitis	Transverse processes of T1 and C7	Between superior and inferior nuchal line of occipital bone	Extension and lateral flexion of head	2.38

Table 4 (Continued)

Trapezius	Heads of clavicles and and spines of scapulae	Occipital bone and thoracie vertebrae	Extension lateral flexion of head	10.6
Sternocleidomastoideus	Head of sternum, medial sections and heads of clavicles	Occipital bone and temporal bone	Lateral flexion and flexion of head	1.6
Levator scapulae	Medical sections of scapulae	Transverse processes of C1, C3	Lateral flexion of neck	17.75
Longus colli	Anterior side of body of C5 anterior side of body of C6 anterior side of body of T1	Anterior side of body of C4 anterior side of body of C3 anterior side of body of C4	Flexion of neck	.75
Scalenus anterior, medius and posterior	Medial clavicle	C3, C4, C5, C6, C7 transverse processes	Flexion and laterial flexion of neck	1.75
Splenius cervicis	T1 spinous process	Transverse processes of C1, C2 C3	Lateral flexion of neck	.7
Longissimus cervicis	T1 transverse processes	Transverse processes of C2, C3, C4, C5, C6	Extension of neck	.6
Spinalis cervicis	Spinous process of T1 and C7	C2 spinous process	Extension of neck	1.25
Semispinalis cervicis	Transverse processes of T2 and C7	Spinous process of C2, C3, C4 and C5	Extension of neck	2.00

Table 5 Specifications on Trunk Musculature

Muscle Group	Origin	Insertion	Action	Cross-Sectional Area (cm^2)
Iliocastalis lumborum	Transverse processes L1-L5	Lower six ribs	Extension and lateral flexion of vertebral column	1.0
Iliocostalis dorsi	Lower six ribs	Upper six ribs	Extension and lateral flexion of vertebral column	.5
Longissimus dorsi	Transverse processes L1-L5	Transverse processes T1-T12	Extension and lateral flexion of vertebral column	1.0
Spinalis dorsi	Spinous processes L2, L1, T12, T11	Spinous processes T4-T8	Extension and lateral flexion of vertebral column	1.0
Semispinalis dorsi	Transverse processes T7-T12	Spinous processes C6, C7, T1, T2, T3	Extension and lateral flexion of vertebral column	1.0
Multifidus	Transverse processes C5-T12	Spinous processes above vertebra of origin	Extension and lateral flexion of vertebral column	1.25
Interspinales	Spinous processes L5-C2	Spinous processes above vertebra of origin	Extension of vertebral column	.5
Intertransversarii	Connect adjacent transverse processes		Lateral flexion of vertebral column	.25

Table 5 (Continued)

External Oblique	Anterior half of iliac crest	Lower 8 ribs	Compresses abdomen	6.85
Internal oblique	Anterior half of iliac crest	Lower 3 ribs and mid line of body	Compresses abdomen	5.68
Rectus abdominus	Pubic symphysis	Xyphoid process	Flexes vertebral column	2.66
Quadratus Lumborum	Iliac crest	Transverse processes L1-L4	Flexes vertebral column	2.8

VII PHASE IV - SIMULATION AND VALIDATION

In Phase IV, the advanced neuromuscular model was validated via simulation of human body responses to high G(lateral) acceleration. Data obtained under similar conditions on air crew personnel experiencing tests in the Dynamic Enviornmental Simualtor at Wright-Patterson AFB, OH, were used for comparison purposes. Some of this data was used in an earlier pilot study developing a trunk musculature (Freivalds, 1984).

The full ATB Model with 15 body segments (head, neck, upper torso, center torso, pelvis, upper arms, lower arms, upper legs, lower legs,and feet) and 14 joints (head junction, neck junction, waist, L_5/s_1, joint, two hips, two knees two ankles, two shoulders, two elbows) was utilized to provide an adequate human neuromusculature. The muscles described in Chapter VI and summarized in Tables 1-5 needed to be added to the existing ATB Model. For each muscle specific coordinates of origin and insertion points were determined form anatomical texts (Quiring et.al., 1945; Quiring, 1947; Gray, 1974; McMinn and Hutchings, 1977). Cross sectional areas obtained from Schumacher and Wolff (1966) and Williams and Belytschlso (1981) were multiplied by the muscular force constant of 100 N/cm^2 (Ikai and Fukunaga, 1968) to determine a muscle force scaling factor. These resulting values were then converted to English units for use in the present ATB Model mode and are summarized in Tables 6-10.

For the simulations of responses to lateral G forces, the body segments were arranged in the semi-reclining posture maintained by air crew personnel in the cockpit. The lower trunk was restrained by a lap belt; any other restrains, such as shoulder pasds or hands placed on controls, were eliminated. Only the neck and trunk musculature on the right side of the body were activated so as to reduce program complexity and execution times. A 2 Gy lateral force was applied

to the body and the acceleration; velocity and displacement of various body segments were recorded.

A graphical response of the whole body reponse (using only trunk and neck musculature) to the lateral force over time is shown in Figure 13. For comparison purposes, the response to a control case with no musculature is given in Figure 12a, while the response using the previous simplified musculature is given in Figure 12b. Although the musculature does not completely prevent the lateral deflection of the body, the response is significantly delayed with head and neck maintaining the upright position for a longer period of time. The result is better observed in Figure 14, which shows the plot of angular displacement of the upper trunk for allthree conditions. At the end of 256 msec the angular displacement is reduced by 20° with the use of musculature. Based on the time history, the response with the musculature lags upto 40 msec behind the control response.

Table 6 ATB Specifications for Elbow Musculature (Right Side Only)

Muscle Group	ORIGIN (in) SEG	X	Y	Z	INSERTION (in) SEG	X	Y	Z	Force Scaling Factor (lbs)
1) Biceps - Short Head	3	1.57	6.28	-3.24	13	.39	.0	-6.56	35.7
Brachii - Long Head	3	.0	6.28	-2.85	13	.39	.0	-6.56	42.4
2) Brachialis	12	.39	.0	-2.68	13	.39	.0	-7.15	101.86
3) Brachioradialis	12	.39	.39	3.61	13	.0	.79	.33	30.14
4) Triceps Medial Head	12	-.39	.0	- .72	13	-.59	.0	-8.53	116.9
Brachii Lateral Head	12	-.39	.0	-1.5	13	-.59	.0	-8.53	115.0
Long Head	3	.0	6.88	-1.85	13	-.59	.0	-8.53	128.4
5) Anconeus	12	.0	1.18	5.19	13	.39	.0	-6.94	20.68
6) Pronator Teres	12	.39	.0	4.35	13	.0	.71	-3.81	35.42
7) Supinator	12	.0	1.18	5.19	13	.0	.59	-5.94	38.94

Table 7 ATB Specifications for Shoulder Musculature (Right Side Only)

Muscle Group	ORIGIN (in) SEG	X	Y	Z	INSERTION (in) SEG	X	Y	Z	Scaling Factor (lbs)
1) Deltoid a)	3	-.79	6.49	-3.81	12	.39	.39	.07	121.11
b)	3	.79	6.49	-3.81	12	.39	.39	.07	121.11
2) Supraspinatus	3	.0	3.74	-1.85	12	.0	1.57	-5.83	72.6
3) Pectoralis a)	3	2.0	.0	-.28	12	.39	.39	-1.9	74.8
Major b)	3	2.0	3.34	-2.64	12	.39	.39	-1.9	74.8
4) Latissimus a)	2	-2.0	.0	3.85	12	.0	.39	-2.68	59.18
Dorsi b)	3	-2.0	.0	.71	12	.0	.39	-2.68	59.18
5) Teres Major	3	.0	4.92	2.09	12	.0	-.39	-3.08	109.34
6) Teres Minor	3	.0	5.71	.51	12	.0	.39	-5.44	34.54
7) Subscapularis	3	.39	4.92	.51	12	.59	.59	-5.44	217.8
8) Coraco Brachialis	3	1.57	7.28	-3.23	12	.0	-.39	-.72	33.44
9) Infraspinatus	3	-.39	4.52	-.28	12	.0	.59	-5.44	131.56

Table 8 ATB Specifications for Hip and Knee Musculature (Right Side Only)

Muscle Group	ORIGIN (in) SEG	X	Y	Z	INSERTION (in) SEG	X	Y	Z	Scaling Factor (lbs)
1) Gluteus Medius	1	-1.46	.0	-2.23	6	-1.97	5.88	-8.21	465.96
2) Gluteus Minimus	1	.0	.0	-1.44	6	-1.18	5.88	-8.21	211.2
3) Tensor Fasciae Latae	1	-1.57	.0	-2.23	6	-1.97	5.49	-5.26	54.56
4) Obturatus Internus	1	.0	1.95	3.68	6	-1.18	3.49	-8.88	86.02
5) Adductor Longus	1	.0	.76	3.28	6	-1.18	4.7	-1.32	110.66
6) Adductor Brevis	1	.0	1.55	3.68	6	-1.18	4.7	-3.09	99.88
7) Adductor Magnus a)	1	.0	3.13	3.68	6	-1.18	4.7	-6.44	226.38
b)	1	.0	1.55	3.68	6	-1.18	4.7	-8.8	226.38
8) Pectineus	1	.787	1.55	.92	6	-1.18	1.0	-5.06	54.34
9) Quadratus Femoris	1	-.79	1.95	3.68	6	-2.36	-1.97	-7.62	64.02
10) Obturatus Externus	1	.0	1.95	3.68	6	-1.18	-1.97	-8.8	108.9
11) Gluteus Maximus a)	1	.0	-3.15	-.65	6	-1.18	1.38	-4.47	323.62
b)	1	.0	.0	.0	6	-1.18	1.38	-4.47	323.62
12) Semimembranosus	1	-1.57	.0	2.49	7	.0	-1.18	-7.14	285.34
13) Semitendinosus	1	-1.97	.0	2.49	7	.39	-.79	-4.39	95.26
14) Biceps Femoris a)	1	-1.77	1.18	2.49	7	.0	1.57	-7.14	129.8
b)	6	-1.18	1.18	-.53	7	.0	1.57	-7.14	129.8
15) Quadriceps a)	1	.0	.0	-.23	7	1.18	.0	-7.93	308.0
b)	6	.0	1.18	.65	7	1.18	.0	-7.93	924.0
16) Iliopsoas a)	1	.0	-.39	3.41	6	-1.18	.79	-6.44	165.66
b)	2	.0	.0	-.17	6	-1.18	.79	-6.44	165.66
17) Gastrocnemius	6	.0	.0	8.52	8	.0	.0	-1.5	344.52
18) Popliteus	6	-1.18	-1.57	9.7	7	-.79	.0	-5.57	43.78
19) Gracilis	1	-.39	.76	3.67	7	.39	-.79	-5.17	35.86
20) Sartorius	1	-1.57	.0	-1.05	7	.39	-.79	-5.17	34.1

Table 9 ATB Specifications for Neck Musculature (Right Side Only)

Muscle Group	ORIGIN (in) SEG	X	Y	Z	INSERTION (in) SEG	X	Y	Z	Scaling Factor (lbs)
1) Longus Capitis	4	-.75	1.0	-.54	5	1.54	.39	3.18	16.5
2) Rectus Capitis Anterior	4	-.75	1.0	-2.52	5	1.26	.39	3.18	5.5
3) Rectus Capitis Lateralis	4	-.75	1.0	-2.52	5	.87	1.18	3.18	5.5
4) Rectus Capitis Posterior Major	4	-.75	.0	-1.86	5	-.55	.94	2.83	11.0
5) Rectus Capitis Posterior Minor	4	-.75	.0	-2.52	5	-.55	.31	2.98	8.47
6) Obliquus capitis Superior	4	-.75	1.0	-2.52	5	-.55	1.38	2.67	22.0
7) Splenius Capitis	4	-.75	.0	2.16	5	-.39	1.57	2.67	26.84
8) Longissimus Capitis	4	-.75	1.0	2.16	5	.08	1.34	2.67	11.0
9) Spinalis Capitis	4	-.75	1.0	2.16	5	-.87	.24	2.83	11.0
10) Semispinalis Capitis	4	-.75	1.0	2.16	5	-1.42	.79	2.67	52.36
11) Trapezius	3	.0	7.28	-2.35	5	-1.42	.39	2.59	233.2
12) Sternocleido-Mastoideus	3	3.0	.0	-2.0	5	-.39	1.57	2.67	35.2
13) Levator Scapulae	3	-2.0	4.28	-1.85	2	-.31	.45	-1.85	390.5
14) Longus Colli	3	.75	.0	-2.0	4	.75	.0	-.18	16.5
15) Scalenus	3	3.0	2.0	-1.85	4	-.75	1.0	.2	38.5
16) Splenius Servicis	3	-.75	.0	-1.26	4	-.75	1.0	-1.86	15.4
17) Longissimus Servicis	3	-.75	1.0	-1.26	4	-.75	1.0	-.54	13.2
18) Spinalis Cervicis	3	-.75	.0	-2.6	4	-.75	.0	-1.86	27.5
19) SemiSpinalis Cervicis	3	-.75	1.0	-2.6	4	-.75	.0	-1.2	44.0

Table 10 ATB Specifications for Trunk Musculature (Right Side Only)

Muscle Group	ORIGIN (in) SEG	X	Y	Z	INSERTION (in) SEG	X	Y	Z	Scaling Factor (lbs)
1) Iliocostalis Lumborum	1	-1.0	1.5	3.85	2	-1.0	3.0	.31	22.0
2) Iliocostalis Dorsi	2	-1.0	3.0	.31	3	-1.0	3.0	.0	11.0
3) Longissimus Dorsi	2	-1.0	1.5	-.19	3	-.75	1.0	.71	22.0
4) Spinalis Dorsi	2	-1.0	.0	-4.23	3	-.75	1.0	.71	22.0
5) Semispinalis Dorsi	3	-.75	1.0	1.89	4	-.75	1.0	1.5	22.0
6) Multifidus a)	2	-1.0	1.5	-2.89	3	-.75	0	4.23	12.75
b)	3	-.75	1.0	-2.04	4	-.75	0	2.82	13.75
7) Interspinales a)	2	1.0	.0	-2.89	3	-.75	0	4.23	5.5
b)	3	-.75	.0	-2.04	4	-.75	0	2.82	5.5
8) Intertrans- a) Versarii	2	-1.0	1.5	-2.89	3	-.75	1.0	4.23	2.75
b)	3	-.75	1.0	-2.04	4	-.75	1.0	2.82	2.75
9) External Oblique	1	3.0	3.52	-3.08	2	.0	3.52	.31	150.7
10) Internal Oblique	1	.0	3.52	-3.08	2	3.0	3.52	.31	124.95
11) Rectus Abdominus	1	1.0	.5	1.92	3	3.0	.5	-4.23	58.52
12) Quadratus Lumborum	1	.0	3.52	-3.08	2	-.75	1.0	-.17	61.6

Fig. 12 - Graphical Display of Trunk Response to Lateral G_Y Forces(2G)

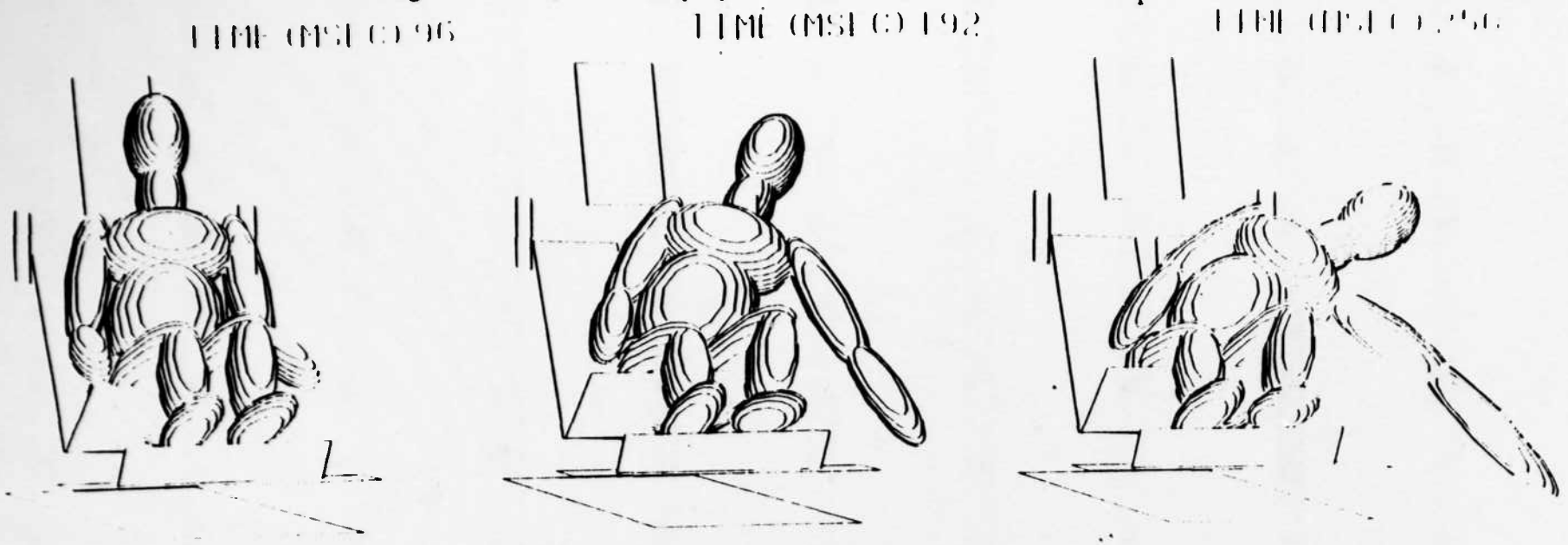

a. Control
b. Neuromusculature (Freivalds, 1984)

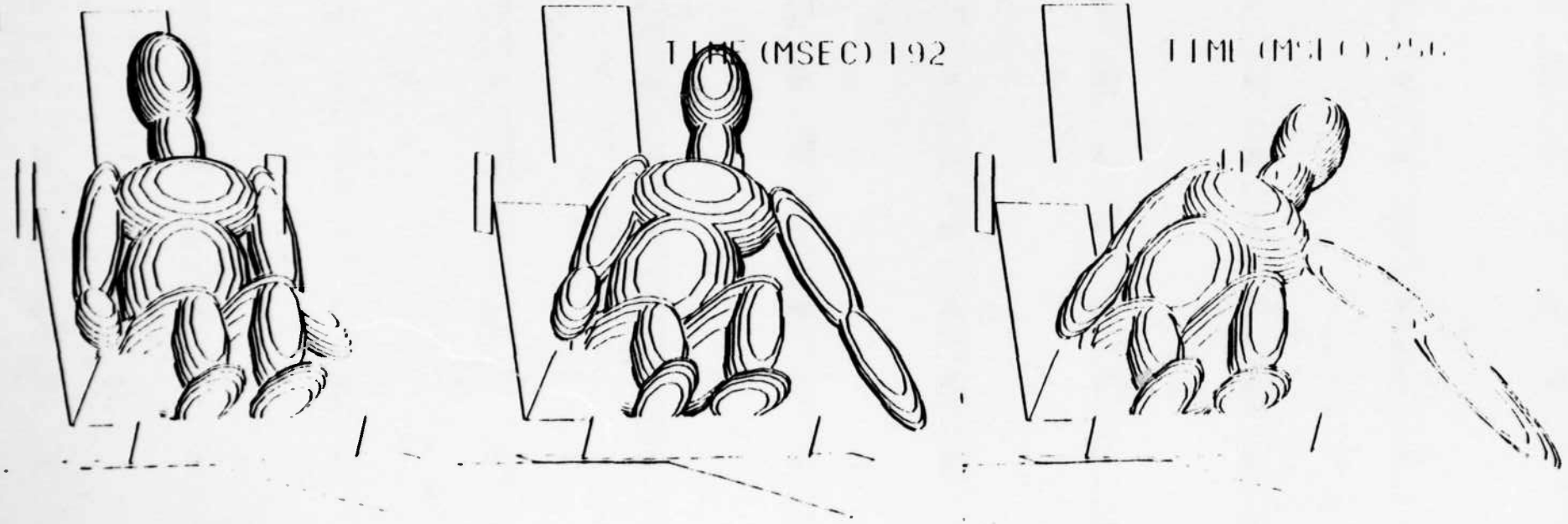

Fig. 13 - Graphical Display of Trunk Response to Lateral G_Y-Forces (2G)
(Current work)

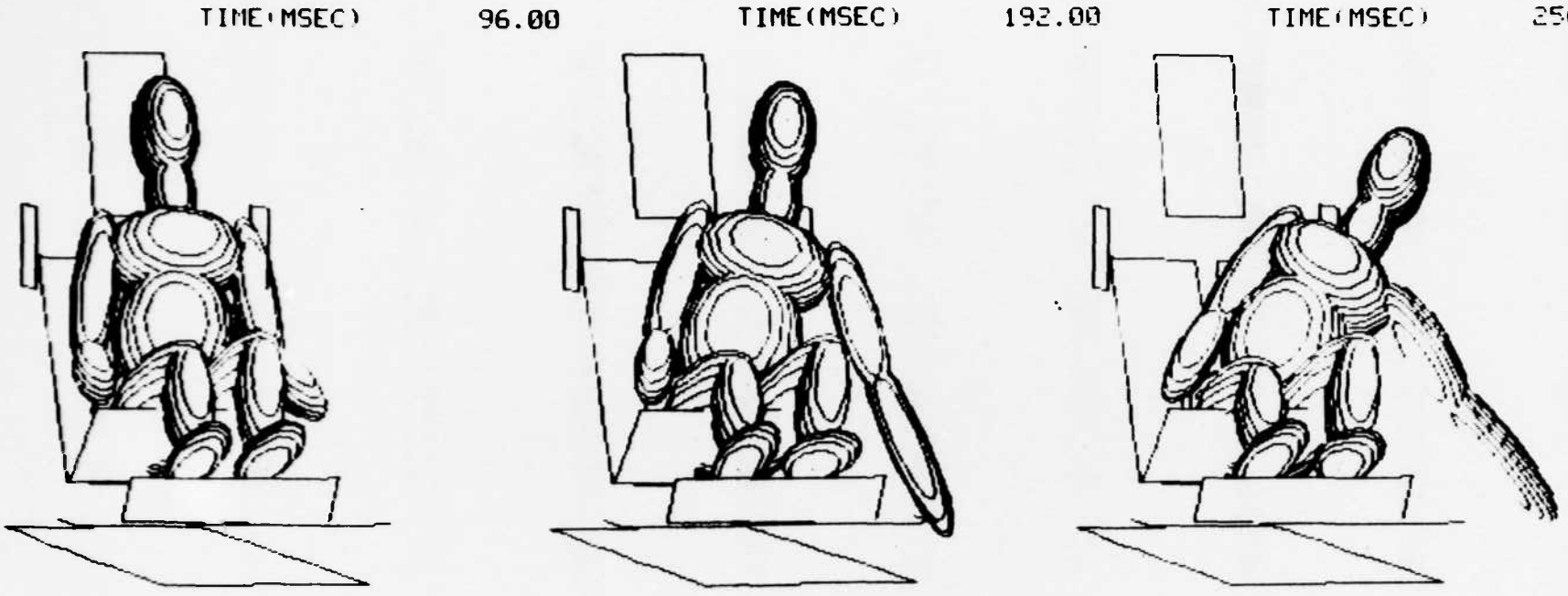

Fig. 14 ANGULAR DISPLACEMENT (ROLL) OF UPPER TRUNK DUE TO LATERAL G-FORCES

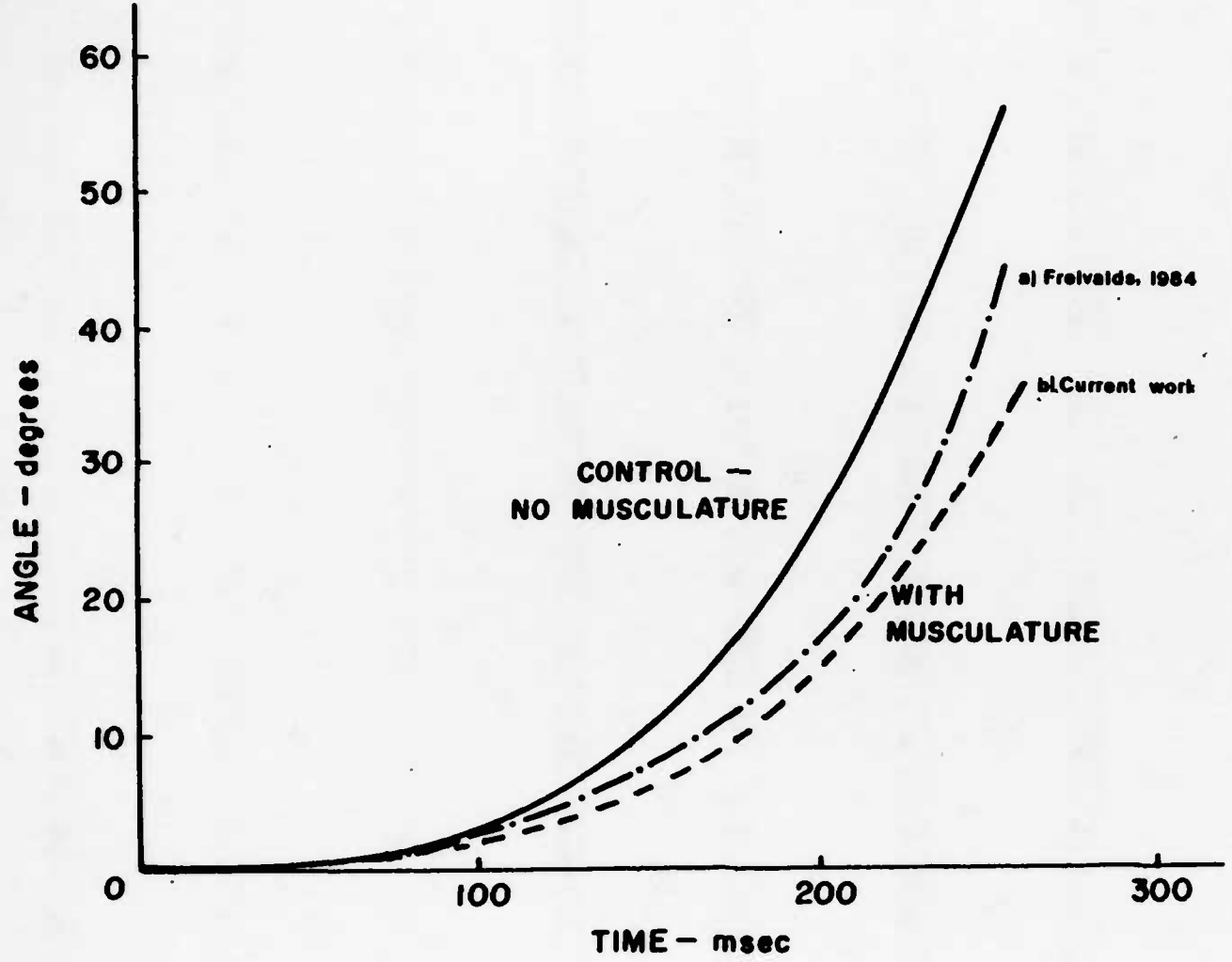

VIII. CONCLUSIONS

Further simulations of various human body motions or responses to external forces need to be conducted in order to more adequately validate the model. These would include not only additional lateral forces, but also forward/back (Gx) and up/down (Gz) forces as well as multidirectional forces. Various combinations of muscle parameter values need to be tested, so as to determine the optimum values for generating the most realistic human response. Similarly, further examination of neuromuscular factors such as reflex arcs may still lead to further improvements in the model. However, the simulations demonstrated that the presently developed muscle model can adequately represent an active human neuromusculature response to dynamic mechanical stresses and can serve as a cost effective research and developmental tool.

REFERENCES

Amis, A. A., D. Dowson and V. Wright, "Elbow Joint Force Predictions for Some Strenuous Isometric Actions," J. Biom., 13:765-775, 1980.

An, K. N., F. C. Hui, B. F. Morrey, R. L. Linscheid, and E. Y. Chao, "Muscles Across the Elbow Joint: A Biomechanical Analysis," J. Biom., 14:659-669, 1981.

Bigland, B. and Lippold, O. C. J. "Motor Unit Activity in the Voluntary Contraction of Human Muscle," J. Physiol., 125:322-335, 1954.

Butler, F. E. and J. T. Fleck, Advanced Restraint System Modelling, AFAMRL-TR-80-14, Wright-Patterson AFB, OH, 1980.

Caldwell, L. S., "Relative Muscle Loading and Endurance," J. Engr. Psychol., Vol. 2:155-161, 1963.

Caldwell, L. S., "The Load-Endurance Relationship for a Static Manual Response," Human Factors, Vol. 6:71-79, 1964.

Chao, E. Y. and B. F. Morrey, "Three Dimensional Rotation of the Elbow," J. Biom., 11:57-73, 1978.

Clamann, H. P., "Activity of Single Motor Units During Isometric Tension," Neurology, 20:254-260, 1970.

Close, R. I., "The Relation between Intrinsic Speed of Shortening and Duration of the Active State of Muscle," J. Physiol., 180:542-559, 1965.

Close, R. I., "Dynamic Properties of Mammalian Skeletal Mucles," Physiol. Rev., 52:129-196, 1972.

Crowninshield, R. D., R. C. Johnston, J. G. Andrews and R. A. Brand, "A Biomechanical Investigation of the Human Hip," J. Biom., 11:75-86, 1978.

Luca, C. J. and W. J. Forrest, "Force Analysis of Individual Muscles acting simultaneously on the shoulder joint during isometric abduction," J. Biom., 6:385-393, 1973.

Dempster, W. T., "Mechanisms of Shoulder Movement," Arch. Phys. Med. and Rehab., 46:49-69, 1965.

Dostal, W. G. and J. C. Andrews, "A Three Dimensional Biomechanical Model of Hip Musculature," J. Biom., 14:803-812, 1981.

Ebashi, S. and Endo, M., "Calcium Ion and Muscular Contraction," Progr. Biophys. Mol. Biol., 18:125-183, 1968.

Engin, A. E., "On the Biomechanics of the Shoulder Complex," J. Biom., 13:575-590, 1980.

Fick, R., Handuch der Anatomie and Mechanik der Gelenke unter Berucksichtigung der bewegenden Muskeln, Jena, Germany; Fischer, 1910.

Fleck, J. T., F. E. Butler, and S. L. Vogel, "An Improved Three Dimensional Computer Simulation of Motor Vehicle Crash Victims," Final Technical Report No. ZQ-5180-L-1, Calspan Corp., 1974, 4 Vols.

Fleck, J. T., "Calspan Three-Dimensional Crash Victim Simulation Program," Aircraft Crashworthiness, University Press of Virginia, 1975.

Fleck, J. T. and F. E. Butler, Developoment of an Improved Computer Model of the Human Body and Extremity Dynamics, AFAMRL-TR-75-14, Wright-Patterson AFB, OH, 1975.

Freivalds, A. Modelling of an Active Neuromuscular Response to Mechanical Stress, AFAMRL-TR-84-XX (in Print)., Wright-Patterson AFB, OH, 1984.

Freivalds, A. and I. Kaleps, "Modelling of Active Neuromuscular Response to Dynamic Mechanical Stresses," Proceedings of the Institute of Industrial Engineers, pp. 196-198, 1983.

Freivalds, A. and I. Kaleps, "Computer-Aided Strength Prediction Using the Articulated Total Body Model," Computer & Industrial Engineering, 8:107-118, 1984.

Fung, Y. C., Biomechanics, Mechanical Properties of Living Tissues, Springer-Verlag, NY, 1981.

Glantz, S. A., "A Constitutive Equation for the Passive Properties of Muscle, J. Biomech., 7:137-145, 1974.

Glantz, S. A., "A Three-Element Description for Muscle With Viscoelastic Passive Elements," J. Biomechanics, 10:5-20, 1977.

Gray, H., T. P. Pick and R. Howden, Anatomy Description and Surgical, (Reprint of 1901 Edition of Gray's Anatomy) Running Press, Philadelphia, 1974.

Hatze, H., "A Theory of Contraction and a Mathematical Model of Striated Muscle," J. Theoret. Biol., 40:219-246, 1973.

Hatze, H. A., "Myocybernetic Control Model of Skeletal Muscle, Biol. Cybernetics, 25:103-119, 1977.

Hatze, H., "A Teleogical Explanation of Weber's Law and the Motor Unit Size Law," Bull Mathem. Biol., 41:407-425, 1979.

Hatze, H., Myocybernetic Control Models of Skeletal Muscle, University of South Africa, Pretoria, 1981.

Huxley, H. E., "Electron Microscope Studies of the Organization of the Filaments in Striated Muscle," Biochem. Biophys. Acta, 12:387, 1953.

Henneman, E. and C. B. Olson, "Relations Between Structure and Function in the Design of Skeletal Muscle," J. Neurophysiol., 28:581-598, 1965.

Ikai, M. and T. Fukunaga, "Calculation of Muscle Strength per Unit Cross-sectional Area of Human Muscle by Means of Ultrasonic Measurement, Int. Z. Angew. Physiol. einschl. Arbeitsphysiol., 26:26-32, 1968.

Jensen, R. H. and D. T. Davy, "An Investigation of Muscle Lines of Action About the Hips: A Centroid Line Approach vs. Straight Line Approach," J. Biom., 8:103-110, 1975.

Kogi, K. and T. Hakamada, "Slowing of Surface Electromyogram and Muscle Strength in Muscle Fatigue," Institute for Science of Labor Reports, Tokyo, Japan, No. 60, 1962.

Kroemer, K. H. E., "Human Strength, Terminology, Measurement, and Interpretation of Data," Human Factors, 12:297-313, 1970.

McMinn, R. M. H. and R. T. Hutchings, Color Atlas of Human Anatomy, Yearbook Medical Publishers, Chicago, IL, 1977.

Merchant, A. C., "Hip Abductor Muscle Force," J. Bone and Jt. Surg., 47A:462-476, 1965.

Milner-Brown, H. S., R. B. Stein and R. Yemm, "The Orderly Recruitment of Human Motor Units During Voluntary Isometric Contractions," J. Physiol., 230:359-370, 1973a.

Milner-Brown, H. S., R. B. Stein, and R. Yemm, "Changes in Firing Rate of Human Motor Units During Linearly Changing Voluntary Contractions," J. Physiol., 230:371-390, 1973b.

Minns, R. J., "Forces at the Knee Joint, Anatomical Considerations," J. Biom., 9:633-643, 1981.

Monod, H. and J. Scherrer, "The Work Capacity of a Synergic Muscular Group," Ergonomics, Vol. 8:329-338, 1965.

Muller, E. A., "Das Arbeitsmaximum bei Statischer Haltearbeit," Arbeitsphysiol, Vol. 5:605-612, 1932.

Nissan, M., "Review of Some Assumption in Knee Biomechanics, J. Biom., 12:375-381, 1980.

Parmley, W. W., L. A. Yeatman and E. H. Sonnenblick, "Differences Between Isotonic and Isometric Force Velocity Reltionships in Cardiac and Skeletal Muscle," Am. J. Physiol, 219:546-550, 1970.

Person, R. and L. P. Kudina, "Discharge Frequency and Discharge Pattern of Human Motor Units During Voluntary Contraction of Muscle," Electroenceph Clin Neurophysiol, 32:471-483, 1972.

Petrofsky, J. S., Isometric Exercise and Its Clinical Implications, C. C. Thomas, Springfield, ILL. 1982.

Quiring, D. P., B. A. Boyle, E. L. Boroush, and B. Lufkin, The Extremities, Lea & Febiger, Philadelphia, 1945.

Quiring, D. P., The Head, Neck and Trunk, Lea & Febiger, Philadelphia, 1947.
Rab, G. T., "Muscle Forces in the Posterior Thoracic Spine," Clin. Orthoped., 139:28-32, 1979.

Rab, G. T., E. Y. S. Chao and R. N. Stauffer, "Muscle Force Analysis of the Lumbar Spine," Orthop. Clincis of North Amer., 8:193-199, 1977.

Rohmert, W., "Ermittlung von Erholungspausen fur Statische Arbeit des Menschen," Int. Z. Angew. Physiol. einschl. Arbeitsphysiol., Vol. 18:123-164, 1960.

Schumacher, G. H. and E. Wolff, "Trockengewicht und Physiologischer Querschnitt der Menschlichen Skelettmuskulatur, II, Physiologische Querschnitte," Anat. Anz., 119:259-269, 1966.

Schutz, R. K., Cyclic Work-Rest Exercises Effect on Continuous Hold Endurance Capacity, Ph.D. Dissertation, University of Michigan, Ann Arbor, MI, 1972.

Seireg, A. and R. J. Arvikar, "A Mathematical Model for Evaluation of Forces in Lower Extremities of the Musculo-skeletal System," J. Biom., 6:313-326, 1973.

Smidt, G. L., "Biomechanical Analysis of Knee Flexion and Extension," J. Biom., 6:79-92, 1973.

Stephens, J. A. and T. P. Usherwood, "The Mechanical Properties of Human Motor Units with Special Reference to Their Fatigability and Recruitment Threshold, Brain Res., 125:91-97, 1977.

Takashima, S. T., S. P. singh, K. A. Harderspeck and A. B. Schultz, "A Model for Semi-quantitative Studies of Muscle Actions, J. Biom., 12:929-939, 1979.

Tanji, J. and M. Kato, "Firing Rate of Individual Motor Units in Voluntary Contraction of Abductor Digiti Minimi Muscle in Man,"Experimental Neurology, 40:771-783, 1973.

Williams, J. and T. Belytschko, A Dynamic Model of the Cervical Spine and Head, AFAMRL-TR-81-5, Wright-Patterson AFB, OH, 1981.

Wismans, J., F. Veldpaus, J. Janssen, A. Huson, P. Struben, "A Three Dimensional Mathematical Model of the Knee Joint, J. Biom., 13:677-685, 1980.

Youm, Y., R. F. Dryer, K. Thambyrajah, A. E. Flatt and B. L. Sprague, "Biomechanical Analyses of Forearm Pronation-supination and Elbow Flexion-extension, J. Biom., 12:245-255, 1979.

END

FILMED

1-85

DTIC